

Exact solutions for a longitudinal steady mixed convection flow over a permeable vertical thin cylinder in a porous medium

E. Magyari ^{a,*}, I. Pop ^b, B. Keller ^a

^a *Chair of Physics of Buildings, Institute of Building Technology, Swiss Federal Institute of Technology (ETH) Zürich, CH-8093 Zürich, Switzerland*

^b *Faculty of Mathematics, University of Cluj, R-3400 Cluj, CP 253, Romania*

Received 22 December 2003; received in revised form 8 September 2004

Available online 19 April 2005

Abstract

The title problem is considered under the assumption that both the surface temperature of the cylinder and the main-stream velocity at the outer edge of the boundary layer vary linearly with the axial distance x from the leading edge. Self-similar solutions are given in exact analytic form. Their domain of existence in the plane (f_w, λ) of the suction/injection parameter f_w and the mixed convection parameter λ is determined. It is shown that in general for both the aiding ($\lambda > 0$) as well as the opposing ($\lambda < 0$) flow regimes multiple solutions bifurcating from certain branching curves of the plane (f_w, λ) occur. The particular case of the dual solutions is discussed in the paper in detail.

© 2005 Elsevier Ltd. All rights reserved.

1. Introduction

Convective flow in fluid-saturated porous media is an area of research undergoing rapid growth in fluid mechanics and heat transfer. This is motivated by a wide range of geophysical and engineering applications including geothermal energy extraction, groundwater resource management, building thermal insulation, enhanced oil recovery, nuclear waste disposal, metal casting (alloy solidification), grain storage, and heat transfer in electronic equipment, among many others. A comprehensive collection of references and reviews of several topics within this broad research area can be

found in the recent books by Nield and Bejan [1], Ingham and Pop [2], Pop and Ingham [3], Vafai [4], and Bejan and Kraus [5].

The Darcian mixed convection flow from a horizontal circular cylinder in a vertical stream was intensively investigated for its applications in many engineering fields. A rich collection of references devoted to this problem can be found in the recent paper by Zhou and Lai [6]. However, the Darcian mixed convection over a vertical circular cylinder in a vertical stream, although also frequently encountered in applications, has received rather little attention. To the authors' best knowledge there are only a few papers addressed to this topic, [7–10]. In this respect, Merkin and Pop [7], have found that for an isothermal cylinder a solution of the boundary layer equation is possible only when $\varepsilon \equiv Ra/Pe \geq -1.354$ and that there is a region of reversed flow when $\varepsilon < -1$. Here $\varepsilon > 0$

* Corresponding author. Tel.: +41 1 633 2867; fax: +41 1 633 1041.

E-mail address: magyari@hbt.arch.ethz.ch (E. Magyari).

Nomenclature

a, b	dimensionless scale factors
f	dimensionless stream function
f_w	suction/injection parameter
g	acceleration due to gravity
h	reduced heat transfer coefficient
K	permeability of the porous medium
L	axial length unit
Pe	Péclet number for a porous medium
r	radial coordinate
r_0	cylinder radius
Ra	Rayleigh number for a porous medium
T	fluid temperature
u, v	velocity components in the x - and r -directions
$U(x)$	mainstream velocity in the axial direction
v_w	velocity of suction or injection in the radial direction
x	axial coordinate

Greek symbols

α_m	equivalent thermal diffusivity
β	coefficient of thermal expansion
γ	curvature parameter
T_0	reference temperature
η	similarity variable
θ	dimensionless temperature
λ	mixed convection parameter
ν	kinematic viscosity
ψ	stream function

Subscripts

w	condition at the wall
∞	condition in the ambient fluid

corresponds to the assisting (hot cylinder) and $\varepsilon < 0$ to the opposing (cold cylinder) flow case, respectively. By Hooper et al. [8] the existence of nonsimilarity solutions has been reported, while by Pop and Na [9] the case of the variable surface heat flux has been investigated in detail. In the paper of Yih [10] the coupled heat and mass transfer has been examined in this context.

In the present paper we consider the problem of similarity solutions for the steady mixed convection boundary layer flow along a permeable semi-infinite thin vertical cylinder embedded in a porous medium by assuming that both the mainstream velocity $U(x)$ and the surface temperature of the cylinder $T_w(x)$ are linear functions of the axial distance x from the leading edge/base of the cylinder,

$$U(x) = U_\infty \frac{x}{L} \quad (1)$$

$$T_w(x) = T_\infty + s_T T_0 \frac{x}{L} \quad (2)$$

The choice of these boundary conditions is motivated on the one hand that the basic equations admit an exact analytical solution for this case (which rarely can be encountered in mixed convection problems in porous media). On the other hand, they apply to several problems of practical interests as e.g. cooling of nuclear reactors during emergency shutdown, cooling of electronic devices by fans, in heat exchangers placed in a low-velocity environment, in solar central receivers exposed to wind currents, etc. No matter how small the externally induced flow is, superimposition of this forced flow needs to be considered, since it can affect the flow structure and total heat transfer significantly.

In Eqs. (1) and (2) L sets the scale of the x axis, $U_\infty > 0$ is the mainstream velocity at the axial distance $x = L$, $T_0 > 0$ is a reference temperature, $T_\infty > 0$ is the ambient temperature of the fluid and $s_T = +1$ corresponds to a hot cylinder ($T_w > T_\infty$, for any $x > 0$) and $s_T = -1$ to a cold cylinder ($T_w < T_\infty$, for any $x > 0$), respectively. Thus, the buoyancy forces aid the development of the boundary layer for $s_T = +1$ and oppose it for $s_T = -1$, respectively. We also allow for a nonvanishing radial velocity at the cylinder surface $v(x, r_0) \equiv v_w(x)$ which proves in this case to be independent of x (see below) such that $v_w < 0$ means suction, $v_w > 0$ injection and $v_w = 0$, corresponds to an impermeable surface for any x , respectively. The paper presents novel exact analytic solutions of this problem and discusses the heat transfer characteristics of the corresponding mixed convection flows in detail.

2. Basic equations

We consider the steady mixed convection flow of a Darcian viscous incompressible fluid along vertical permeable cylinder of radius r_0 embedded in a fluid-saturated porous medium of constant ambient temperature T_∞ under the assumption that the mainstream velocity is given by Eq. (1) (see Fig. 1). The governing equations, namely the equation of continuity, the Darcy equation with Boussinesq approximation and the energy equation in the usual boundary-layer approximation are of the form (see e.g. [1,2,7])

$$\frac{\partial}{\partial x}(ru) + \frac{\partial}{\partial r}(rv) = 0 \quad (3)$$

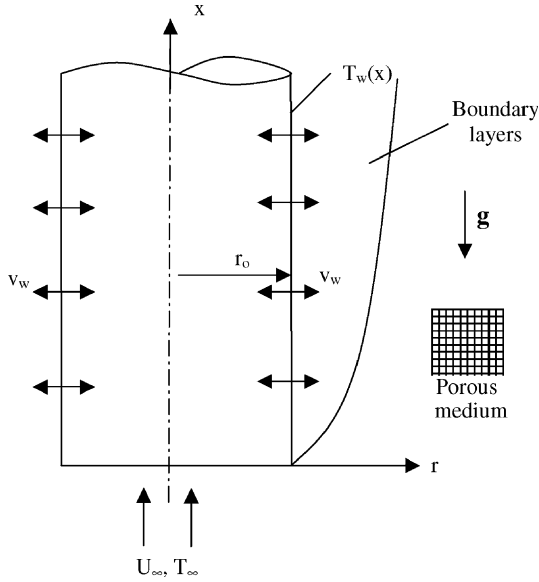


Fig. 1. Geometry and flow and temperature boundary layer domain.

$$u = U(x) + \frac{g\beta K}{\nu}(T - T_\infty) \tag{4}$$

$$u \frac{\partial T}{\partial x} + v \frac{\partial T}{\partial r} = \alpha_m \left(\frac{\partial^2 T}{\partial r^2} + \frac{1}{r} \frac{\partial T}{\partial r} \right) \tag{5}$$

The coordinates $x \geq 0$ and $r \geq r_0$ measure distances along the surface and normal to it respectively, u and v are the velocity components along x and r axes, $T(x, r)$ is the fluid temperature, g is the acceleration due to gravity, K is the permeability of the porous medium, ν is the kinematic viscosity and α_m is the effective thermal diffusivity. The boundary condition to be applied to Eqs. (3)–(5) are

$$v = v_w(x), \quad T = T_w(x) \quad \text{on } r = r_0 \tag{6}$$

$$u \rightarrow U(x), \quad T \rightarrow T_\infty \quad \text{as } r \rightarrow \infty \tag{7}$$

where $v_w < 0$ for suction, $v_w > 0$ for injection and $v_w = 0$ for an impermeable surface, respectively.

It should be mentioned that flow over cylinders is considered to be two-dimensional if the body radius is large compared to the boundary layer thickness. For a thin or slender cylinder, the radius of the cylinder may be of the same order as the boundary layer thickness. Therefore, the flow may be considered as axisymmetric instead of two-dimensional. In this case, the governing Eqs. (3) and (5) contain the transverse curvature term which influences both the velocity and temperature fields. The effect of the transverse curvature is important in some practical applications such as wire or fibre drawing where accurate prediction of flow and heat transfer is required and thick boundary layer can exist on slender or near slender bodies.

3. Similarity transformation

We first define the stream function ψ in the usual way, $u = r^{-1} \partial \psi / \partial r$, $v = -r^{-1} \partial \psi / \partial x$ and then perform the similarity transformation

$$\begin{aligned} \psi &= 2a\alpha_m x f(\eta) \\ \eta &= b \frac{r^2 - r_0^2}{r_0^2} \end{aligned} \tag{8}$$

$$T = T_\infty + s_T T_0 \frac{x}{L} \theta(\eta)$$

Thus, with the choice of the axial length unit L as

$$L = \frac{U_\infty r_0^2}{4\alpha_m a b} \tag{9}$$

Eqs. (3)–(5) reduce to the following ordinary differential equations

$$f' = 1 + \lambda \theta \tag{10}$$

$$(\eta + b)\theta'' + \theta' + a(f\theta' - f'\theta) = 0 \tag{11}$$

In the above equations a and b are dimensionless scale factors of ψ and η , respectively, and

$$\lambda = s_T \frac{Ra}{Pe} \tag{12}$$

denotes the mixed convection parameter. The (positive) Rayleigh and Péclet numbers are defined as

$$Ra = \frac{g\beta K T_0 L}{\alpha_m \nu} \quad \text{and} \quad Pe = \frac{U_\infty L}{\alpha_m} \tag{13}$$

respectively, and the primes denote differentiation with respect to η .

The system of Eqs. (10) and (11) has to be solved along with the boundary conditions

$$f(0) = f_w, \quad \theta(0) = 1, \quad \theta(\eta)|_{r \rightarrow \infty} \rightarrow 0 \tag{14}$$

where f_w denotes the suction/injection parameter.

In terms of the solution of this boundary value problem, the velocity field is obtained in the form

$$\begin{aligned} u(x, r) &= U(x) \cdot f'(\eta) \\ v(x, r) &= -\frac{2a\alpha_m}{r} f(\eta) \end{aligned} \tag{15}$$

Therefore, in the present problem the radial velocity at the surface of the cylinder is independent of the axial coordinate x ,

$$v_w(x) = -\frac{2a\alpha_m}{r_0} f_w \tag{16}$$

4. Exact solution

Eqs. (10) and (11) subject to the boundary conditions (14) admit the exact solution

$$\theta(\eta) = e^{-a\eta} \tag{17}$$

$$f(\eta) = f_w + \eta + \frac{\lambda}{a}(1 - \theta) \tag{18}$$

where

$$a\eta = ab \frac{r^2 - r_0^2}{r_0^2}, \quad ab > 0 \tag{19}$$

This solution is valid if the scale factors a and b satisfy (in addition to $ab > 0$) the equation

$$a(b - f_w) - (\lambda + 2) = 0 \tag{20}$$

The corresponding dimensional velocity components and the temperature field are then given by

$$u(x, r) = U_\infty \frac{x}{L} \cdot (1 + \lambda e^{-a\eta}) \tag{21}$$

$$v(x, r) = -\frac{2a\alpha_m}{r} \left[f_w + \eta + \frac{\lambda}{a}(1 - e^{-a\eta}) \right] \tag{22}$$

$$T(x, r) = T_\infty + s_T T_0 \frac{x}{L} e^{-a\eta} \tag{23}$$

The radial wall heat flux is obtained as

$$q_w(x) = 2s_T ab \frac{k_m T_0}{L} \frac{x}{r_0} \tag{24}$$

where k_m stands for the effective thermal conductivity of the saturated porous medium.

5. Discussion

The present problem possesses two basic length scales, a radial and an axial one. A natural unit of a yardstick which measures the radial distances (from the cylinder surface) is obviously the cylinder radius r_0 . The unit L of the yardstick which measures the axial distances (from the cylinder base/leading edge, $x = 0$) represents according to Eq. (1) the distance x at which the mainstream velocity takes the (arbitrarily) prescribed value U_∞ . Thus, according to Eq. (2), the reference temperature T_0 is specified in terms of the ambient temperature T_∞ and the (arbitrarily) prescribed wall temperature T_w at $x = L$ as $T_0 = s_T(T_w(L) - T_\infty)$.

Obviously, the yardsticks measuring the radial and axial distances can be chosen arbitrarily. This physical circumstance manifests itself in the presence of the scale factors a and b in Eq. (9) which relates the two basic length scales to each other. For given values of f_w and λ , the values of the two scale factors a and b are restricted (in addition to $ab > 0$) by a single equation, Eq. (20), only. Now, if we parametrize a and b by an arbitrary (real) parameter, say γ , which will be referred to hereafter as length to curvature ratio, i.e. if we put in Eq. (20) $a = a(\gamma)$ and $b = b(\gamma)$, we obtain for γ the equation

$$a(\gamma)[b(\gamma) - f_w] - (\lambda + 2) = 0 \tag{25}$$

Obviously, it is always possible to choose the functions $a = a(\gamma)$ and $b = b(\gamma)$ in such a way that Eq. (25) admits arbitrarily many solutions $\gamma = \gamma_n$, which all satisfy the condition $a(\gamma_n) \cdot b(\gamma_n) > 0$ and in some domain of the parameter plane (f_w, λ) all of them are real and distinct. In this way, Eq. (17) yields n (in general distinct) solutions for θ ,

$$\theta \equiv \theta_n(\eta) = \exp \left[-a(\gamma_n) \cdot b(\gamma_n) \frac{r^2 - r_0^2}{r_0^2} \right] \tag{26}$$

We may conclude, therefore, that in the present mixed convection problem always multiple solutions are possible. Their physical origin resides in fact in a ‘‘scaling freedom’’, i.e. in the freedom to choose arbitrarily the axial and radial length scales (i.e. the ‘‘length to curvature ratio’’ of the cylinder), according to our wish. In other words, by watching the flow on the x and r scales which are related to each other according to equation

$$L \equiv L_n = \frac{U_\infty r_0^2}{4\alpha_m a(\gamma_n) b(\gamma_n)} \tag{27}$$

we will see in general quite different flow and heat transfer characteristics for the one and the same values of the physical parameters f_w and λ . Thus, the radial 1% width $\delta_{r,n}$ of the dimensionless temperature profiles (26), and the corresponding radial surface heat flux $q_{w,n}(x)$ are given by equations

$$\delta_{r,n} = r_0 \cdot \sqrt{1 + \frac{2 \ln 10}{a(\gamma_n) b(\gamma_n)}} \tag{28}$$

and

$$\begin{aligned} q_{w,n}(x) &= 2s_T a(\gamma_n) b(\gamma_n) \frac{k_m T_0}{L_n} \frac{x}{r_0} \\ &= 8s_T a^2(\gamma_n) b^2(\gamma_n) \frac{\alpha_m k_m T_0}{U_\infty r_0^3} x \end{aligned} \tag{29}$$

respectively.

In order to be more specific, we consider a simple example in which Eq. (25) is an algebraic equation of second degree in γ such that (at most) dual solutions can arise. To this end we choose

$$a(\gamma) = b(\gamma) \equiv \frac{1}{\gamma} \tag{30}$$

In this case $a(\gamma_n) b(\gamma_n) = 1/\gamma_n^2 > 0$ is automatically satisfied for any real solution γ_n of Eq. (25) which now becomes

$$\frac{1}{\gamma^2} - f_w \frac{1}{\gamma} - (\lambda + 2) = 0 \tag{31}$$

The solutions of Eq. (31) are

$$\frac{1}{\gamma_\pm} = \frac{1}{2} \left(f_w \pm \sqrt{f_w^2 + 4\lambda + 8} \right) \tag{32}$$

The length scales on which the corresponding solutions (21)–(23) can be watched are

$$L_{\pm} = \frac{U_{\infty} r_0^2}{4\alpha_m} \gamma_{\pm}^2 = \frac{U_{\infty} r_0^2}{\alpha_m} \left(f_w \pm \sqrt{f_w^2 + 4\lambda + 8} \right)^{-2} \quad (33)$$

It is worth mentioning here that our parameter γ which connects the axial and radial length units L and r_0 to each other according to Eq. (33), is equivalent in fact to the “curvature parameter” β introduced by Mahmood and Merkin [11] in their investigation of the mixed convection of a clear viscous fluid over a vertical cylinder under the same conditions (1) and (2). In the present notation their β is connected to our length to curvature ratio γ occurring in $4\alpha_m L = U_{\infty} r_0^2 \gamma^2$ by the relationship $\gamma = 2(\alpha_m/\nu)^{1/2} \beta$.

In terms of γ_{\pm} the temperature profiles (26), the radial surface heat fluxes (29) and the velocity components (21) and (22) become,

$$\theta_{\pm}(\eta) = \exp \left[-\frac{r^2 - r_0^2}{\gamma_{\pm}^2 r_0^2} \right] = \exp \left[\frac{1}{4} \left(f_w \pm \sqrt{f_w^2 + 4\lambda + 8} \right)^2 \left(1 - \frac{r^2}{r_0^2} \right) \right] \quad (34)$$

$$q_{w,\pm}(x) = \frac{S_T}{\gamma_{\pm}^4} \frac{8\alpha_m k_m T_0}{U_{\infty} r_0^3} x \quad (35)$$

$$u_{\pm}(x, r) = U_{\infty} \frac{x}{L_{\pm}} [1 + \lambda \theta_{\pm}(\eta)] \quad (36)$$

$$v_{\pm}(x, r) = -\frac{2\alpha_m}{r} \left[\frac{f_w}{\gamma_{\pm}} - \frac{1}{\gamma_{\pm}^2} \left(1 - \frac{r^2}{r_0^2} \right) + \lambda(1 - \theta_{\pm}) \right] \quad (37)$$

The existence domain of the solutions corresponding to the parametrization (30) of the scale factors a and b is the region of the parameter plane (f_w, λ) where

$$\lambda \geq \lambda_{\text{crit}}(f_w) = -2 - \frac{f_w^2}{4} \quad (38)$$

holds, except for the point $(f_w, \lambda) = (0, -2)$ which is excluded (see Fig. 2). Thus, Eq. (32) can be rewritten as

$$\frac{1}{\gamma_{\pm}} = \frac{f_w}{2} \pm \sqrt{\lambda - \lambda_{\text{crit}}} \quad (39)$$

Below the critical parabola (38) no solutions of type (17)–(19) exist.

With each of the (nonvanishing) roots $1/\gamma_{\pm}$ of Eq. (31) corresponding to a given point (f_w, λ) of the existence domain (the gray field of Fig. 1) there is associated a solution (21)–(23) of our boundary value problem. Thus, to any point (f_w, λ) of the existence domain there correspond *dual solutions*, except for the line $\lambda = -2$ on which (for $f_w \neq 0$) a unique solution exists. This unique solution is:

$$\gamma = \frac{1}{f_w}, \quad L = \frac{U_{\infty} r_0^2}{4\alpha_m f_w^2}, \quad \lambda = -2, \quad f_w \neq 0 \quad (40)$$

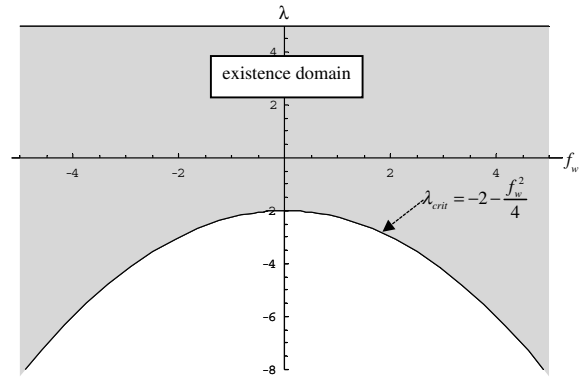


Fig. 2. The gray field of the parameter plane (f_w, λ) above the critical parabola (38) represents the existence domain of the exact solutions (21)–(23) corresponding to the parametrization (30) of the scale factors a and b . Positive and negative values of λ correspond to aiding and opposing flow regimes, respectively. The points of the critical parabola, except for $(f_w, \lambda) = (0, -2)$, also belong to this domain.

$$\theta(\eta) = \exp \left[f_w^2 \left(1 - \frac{r^2}{r_0^2} \right) \right] \quad (41)$$

$$u(x, r) = U_{\infty} \frac{x}{L} [1 - 2\theta(\eta)] \quad (42)$$

$$v(x, r) = -\frac{2\alpha_m}{r} \left[f_w^2 \frac{r^2}{r_0^2} - 2(1 - \theta) \right] \quad (43)$$

$$\delta_r = r_0 \cdot \sqrt{1 + \frac{2}{f_w^2} \ln 10} \quad (44)$$

$$q_w(x) = 8S_T f_w^4 \frac{\alpha_m k_m T_0}{U_{\infty} r_0^3} x \quad (45)$$

The line $\lambda = -2 (f_w \neq 0)$ is in fact a singular line where one of the dual solutions, namely that corresponding to the root $1/\gamma = 0$ of Eq. (31), “disappears” from the finite scale of our length to curvature ratio γ . The second root of Eq. (31), $1/\gamma = f_w$ specifies then the above “unique solution” (40)–(45).

For the points of the λ -axis above of $\lambda = -2$ and for the points of the critical parabola (except for $(f_w, \lambda) = (0, -2)$) the dual solutions become coincident, i.e. they appear in these cases as quasi unique solutions of our boundary value problem. In the former case (i.e. for $\lambda > -2, f_w = 0$) these coincident solutions are

$$\gamma_+ = -\gamma_- \equiv \gamma = (\lambda + 2)^{-1/2},$$

$$L_+ = L_- \equiv L = \frac{U_{\infty} r_0^2}{4\alpha_m (\lambda + 2)}, \quad \lambda > -2, \quad f_w = 0 \quad (46)$$

$$\theta_+(\eta) = \theta_-(\eta) \equiv \theta(\eta) = \exp \left[(\lambda + 2) \left(1 - \frac{r^2}{r_0^2} \right) \right] \quad (47)$$

$$u_+(x, r) = u_-(x, r) \equiv u(x, r) = U_\infty \frac{x}{L} [1 + \lambda \theta(\eta)] \quad (48)$$

$$v_+(x, r) = v_-(x, r) \equiv v(x, r) = \frac{2\alpha_m}{r} \left[(\lambda + 2) \left(1 - \frac{r^2}{r_0^2} \right) - \lambda(1 - \theta) \right] \quad (49)$$

$$\delta_{r,+} = \delta_{r,-} \equiv \delta_r = r_0 \cdot \sqrt{1 + \frac{2 \ln 10}{\lambda + 2}} \quad (50)$$

$$q_{w,+}(x) = q_{w,-}(x) \equiv q_w(x) = 8s_T(\lambda + 2)^2 \frac{\alpha_m k_m T_0}{U_\infty r_0^3} x \quad (51)$$

The coincident solutions corresponding to the points of the critical parabola (except for the point $(f_w, \lambda) = (0, -2)$) are of the form

$$\gamma_+ = \gamma_- \equiv \gamma = \frac{2}{f_w}, \quad L_+ = L_- \equiv L = \frac{U_\infty r_0^2}{\alpha_m f_w^2}, \quad \lambda = \lambda_{crit}, \quad f_w \neq 0 \quad (52)$$

$$\theta_+(\eta) = \theta_-(\eta) \equiv \theta(\eta) = \exp \left[\frac{f_w^2}{4} \left(1 - \frac{r^2}{r_0^2} \right) \right] \quad (53)$$

$$u_+(x, r) = u_-(x, r) \equiv u(x, r) = U_\infty \frac{x}{L} [1 + \lambda_{crit} \theta(\eta)] \quad (54)$$

$$v_+(x, r) = v_-(x, r) \equiv v(x, r) = -\frac{\alpha_m}{r} \left[f_w^2 - \frac{f_w^2}{2} \left(1 - \frac{r^2}{r_0^2} \right) + 2\lambda_{crit}(1 - \theta) \right] \quad (55)$$

$$\delta_{r,+} = \delta_{r,-} \equiv \delta_r = r_0 \cdot \sqrt{1 + \frac{8}{f_w^2} \ln 10} \quad (56)$$

$$q_{w,+}(x) = q_{w,-}(x) \equiv q_w(x) = \frac{S_T}{2} f_w^4 \frac{\alpha_m k_m T_0}{U_\infty r_0^3} x \quad (57)$$

It is also of interest to specify where in their existence domain the dual solutions are realized by a lateral suction or injection of the liquid, respectively. The answer is shown in Fig. 3 and has been obtained by the following considerations.

According to Eq. (37), the radial velocity at the cylinder surface is now given by

$$v_{w,\pm} = -\frac{2\alpha_m}{r_0} \frac{f_w}{\gamma_\pm} \quad (58)$$

Thus, we have (for $f_w \neq 0$):

- suction if $\text{sgn}(f_w) = \text{sgn}(\gamma_n)$ (59)

- injection if $\text{sgn}(f_w) = -\text{sgn}(\gamma_n)$ (60)

On the other hand, the sum S and the product P of the roots $1/\gamma_\pm$ of Eq. (31) are given in terms of f_w and λ by the relationships

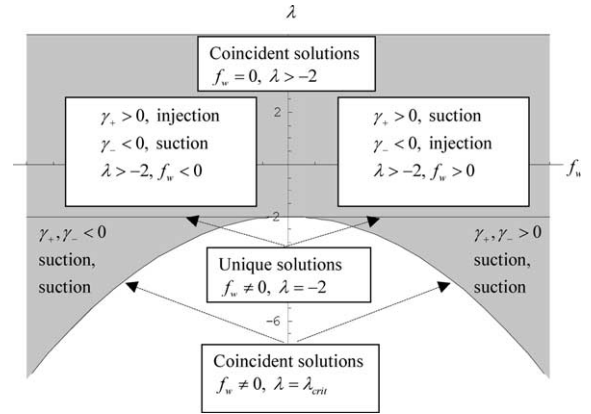


Fig. 3. The unique, dual and coincident character of the exact solutions in their existence domain and how these are associated with the corresponding lateral suction/injection velocities of the fluid.

$$S \equiv \frac{1}{\gamma_+} + \frac{1}{\gamma_-} = f_w \quad (61)$$

$$P \equiv \frac{1}{\gamma_+} \cdot \frac{1}{\gamma_-} = -(\lambda + 2)$$

Taking into account Eqs. (58)–(61) one easily deduces that the dual solutions are realized by suction or injection according to the following schematics (see Fig. 3):

$$f_w > 0 : \begin{cases} \left\{ \begin{array}{l} \gamma_+ > 0, \text{ suction} \\ \gamma_- > 0, \text{ suction} \end{array} \right\} & \text{as } \lambda_{crit} < \lambda < -2 \\ \left\{ \begin{array}{l} \gamma_+ > 0, \text{ suction} \\ \gamma_- < 0, \text{ injection} \end{array} \right\} & \text{as } \lambda > -2 \end{cases} \quad (62)$$

$$f_w < 0 : \begin{cases} \left\{ \begin{array}{l} \gamma_+ < 0, \text{ suction} \\ \gamma_- < 0, \text{ suction} \end{array} \right\} & \text{as } \lambda_{crit} < \lambda < -2 \\ \left\{ \begin{array}{l} \gamma_+ > 0, \text{ injection} \\ \gamma_- < 0, \text{ suction} \end{array} \right\} & \text{as } \lambda > -2 \end{cases} \quad (63)$$

In order to be specific, in Fig. 4 the branching curve (39) of the dual solutions is shown as a function of the mixed convection parameter λ for $f_w = +2$, which implies $\lambda_{crit} = -3$. As a further illustration, in Fig. 5 the dual temperature profiles (34) as functions of the radial distance $r \geq r_0$ are plotted for $(f_w, \lambda) = (2, -0.5)$ and $r_0 = 1$. The upper and lower branch solutions correspond to the γ values $\gamma_+ = 0.38742$ and $\gamma_- = -1.72076$, and can be realized by a lateral suction and injection of the fluid with velocity $v_{w,+} = -4\alpha_m/(r_0\gamma_+) < 0$ and $v_{w,-} = -4\alpha_m/(r_0\gamma_-) > 0$, respectively.

As the expression (21) of the exact solution for the axial velocity component $u(x, r)$ shows, in the opposing

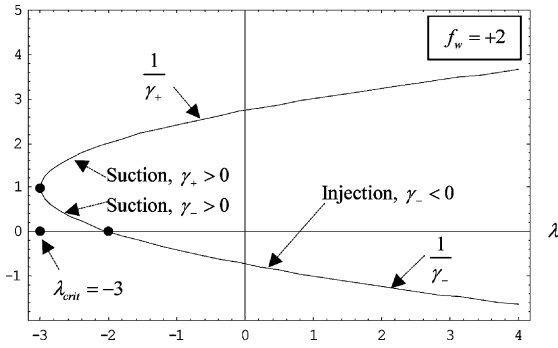


Fig. 4. The branching curve (39) of the dual solutions as a function of the mixed convection parameter λ for $f_w = +2$. In this case $\lambda_{crit} = -3$. Our exact dual solutions can be realized both in the aiding ($\lambda > 0$) and in the opposing ($\lambda_{crit} < \lambda < 0$, $\lambda \neq -2$) flow regimes, respectively.

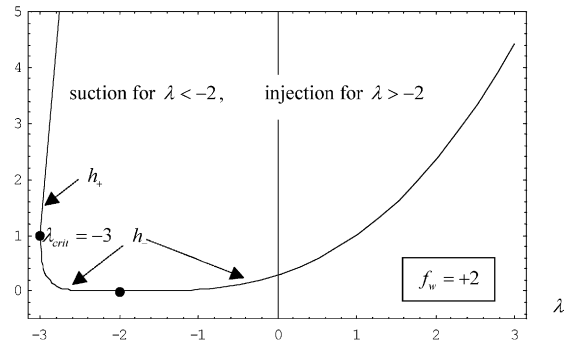


Fig. 6. The heat transfer coefficient (65) of the dual solutions plotted as a function of the mixed convection parameter λ for $f_w = +2$.

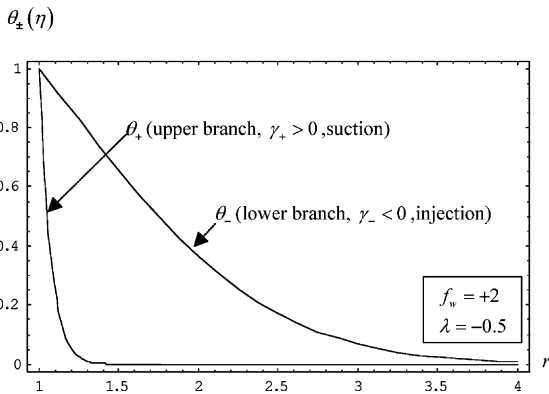


Fig. 5. The dual temperature profiles (34) as functions of the radial distance $r \geq r_0$ are plotted for $(f_w, \lambda) = (2, -0.5)$ and $r_0 = 1$. The upper and lower branch solutions correspond to the γ values $\gamma_+ = 0.38742$ and $\gamma_- = -1.72076$, and can be realized by a lateral suction and injection, respectively.

flow regime $\lambda < 0$ in the neighborhood of the cylinder surface backflow ($u \uparrow U$) can occur if $\lambda_{crit} \leq \lambda < -1$. At the radial distance(s)

$$r_* = r_0 \cdot \sqrt{1 + \frac{\ln |\lambda|}{a(\gamma)b(\gamma)}} = r_0 \cdot \sqrt{1 + \gamma_{\pm}^2 \ln |\lambda|}, \quad \lambda_{crit} \leq \lambda < -1 \quad (64)$$

where the axial velocity component vanishes, the backflow changes then to a forward flow regime ($u \uparrow U$).

Finally, as shown by Eq. (35) the radial wall heat flux depends on the length to curvature ratio γ sensitively. As an illustration of this dependence, in Fig. 6 the heat transfer coefficient

$$h_{\pm} \equiv s_T \frac{U_{\infty} f_0^3}{8\alpha_m k_m T_0} \frac{q_{w,\pm}(x)}{x} = \frac{1}{\gamma_{\pm}^4} \quad (65)$$

is plotted as a function of the mixed convection parameter λ for $f_w = +2$. The value of h_+ or h_- gives for a specified value of λ the heat transferred from the cylinder surface to the fluid if $\lambda > 0$ (direct heat flux) or from the fluid to the surface if $\lambda < 0$ (reversed heat flux), respectively.

6. Summary and conclusions

Exact analytic solutions for a steady mixed convection boundary layer flow over a permeable vertical cylinder have been obtained in this paper. It has been shown that multiple solutions can arise both in the aiding as well as in the opposing flow regimes of the problem. The simple form of the solutions allows a deep insight into the physical origin of the multiple solutions encountered. These multiple solutions being obtained from one and the same analytic expression and for the same values of f_w and λ but for different choices of the length-to-curvature-ratio of the cylinder, we arrive at the conclusion that the physical origin of the multiplicity resides simply in our freedom to choose the axial and radial length scales arbitrarily. In other words, the occurrence of the multiple solutions (at least in the present case) is a subtle length scale effect.

References

- [1] D.A. Nield, A. Bejan, Convection in Porous Media, second ed., Springer, New York, 1999.
- [2] D.B. Ingham, I. Pop (Eds.), Transport Phenomena in Porous Media, vol. 2, Pergamon, Oxford, 2002.
- [3] I. Pop, D.B. Ingham, Convective Heat Transfer: Computational and Mathematical Modelling of Viscous Fluids and Porous Media, Pergamon, Oxford, 2001.
- [4] K. Vafai (Ed.), Handbook of Porous Media, Marcel Dekker, New York, 2000.

- [5] A. Bejan, A.D. Kraus (Eds.), *Heat Transfer Handbook*, Wiley, New York, 2003.
- [6] M.J. Zhou, F.C. Lai, Aiding and opposing mixed convection from a cylinder in a saturated porous medium, *J. Porous Media* 5 (2002) 103–111.
- [7] J.H. Merkin, I. Pop, Mixed convection boundary-layer on a vertical cylinder embedded in a saturated porous medium, *Acta Mech.* 66 (1987) 251–262.
- [8] W.B. Hooper, T.S. Chen, B.F. Armaly, Mixed convection along an isothermal vertical cylinder in porous media, *AIAA J. Thermophys. Heat Transfer* 8 (1994) 92–99.
- [9] I. Pop, T.-Y. Na, Darcian mixed convection along slender vertical cylinders with variable surface heat flux embedded in a porous medium, *Int. Commun. Heat Mass Transfer* 25 (1998) 251–260.
- [10] K.A. Yih, Coupled heat and mass transfer in mixed convection about a vertical cylinder in a porous medium: the entire regime, *Mech. Res. Commun.* 25 (1998) 623–630.
- [11] T. Mahmood, J.H. Merkin, Similarity solutions in axisymmetric mixed-convection boundary-layer flow, *J. Eng. Math.* 22 (1988) 73–92.